

Effects of polarization and permittivity gradients and other parameters on the anomalous vertical shift behavior of graded ferroelectric thin films

Y. Zhou^{a)}

Department of Applied Physics, The Hong Kong Polytechnic University, Hong Kong, China

H. K. Chan

School of Physics and Astronomy, The University of Manchester, Manchester M13 9PL, United Kingdom

C. H. Lam and F. G. Shin

Department of Applied Physics, Materials Research Center and Center for Smart Materials, The Hong Kong Polytechnic University, Hong Kong, China

(Received 18 May 2005; accepted 14 June 2005; published online 9 August 2005)

We studied theoretically the dependence of the “polarization offset” on various parameters in compositionally graded ferroelectric thin films. Our model adopts the Landau-Khalatnikov equation to describe hysteresis behavior and takes the time-dependent space-charge-limited conductivity into account to investigate the effects of polarization and permittivity gradients, charge mobilities, and thickness in graded ferroelectric thin films. We found that both polarization and permittivity gradients are requisite for the occurrence of offset phenomena. It is also found that larger gradients of remanent polarization and permittivity, a smaller thickness, and a larger charge mobility can generally enhance the effect of vertical offsets. The qualitative agreement between simulation and experiment further supports our previous notion that the asymmetric conduction current arising as a result of the composition gradient is an important factor leading to the polarization offset phenomenon. © 2005 American Institute of Physics. [DOI: 10.1063/1.1996833]

I. INTRODUCTION

The “graded ferroelectrics” have attracted great research interest for many years because of its uncommon physical properties. The unconventional behavior presented by such heterogeneous ferroelectric systems is thought to arise from the polarization nonuniformity imposed by a composition, temperature, or stress gradient.¹⁻³ One of the most notable phenomenon is the large polarization offset along the vertical axis found in the hysteresis loop measurements. Values as large as $420 \mu\text{C}/\text{cm}^2$ were reported for the polarization offset in lead-zirconate-titanate (PZT) graded structures.⁴ These offsets have been reported to have a strong temperature dependence, giving rise to possible pyroelectric applications in addition to other potential sensor, actuator, and energy converter applications. On the other hand, recent results have shown the polarization offsets in graded PZT to be sensitive to the ambient oxygen concentration, giving rise to possible oxygen sensor applications.⁵ Theoretical models have played key roles in providing deeper insight, and different approaches have been proposed. The offset has been interpreted as a static polarization developed across the ferroelectric film under the application of an alternating voltage. Recently it was suggested that very large offsets are unphysical and they have to be corrected with the ratio between the sample capacitance and that of the reference or loading capacitance.

Another suggested origin of the polarization offset is the possible asymmetry in the leakage current which gives a sort of diode effect. Thus, although a number of distinct groups have reported on the anomalous hysteretic behavior of the graded ferroelectric structures, none of the suggested models can give a convenient explanation for the polarization offset occurrence.

On the other hand, it is widely reported that the offset magnitudes and directions are strongly dependent on the composition or temperature gradient. It is suggested that the polarization offsets are composition or temperature dependent through the polarization and dielectric constants of the graded materials.⁶ The offsets also display a dependence on the applied electric field. However, so far only very few experimental and theoretical investigations have been performed to study the interplay of the effects of ferroelectric and dielectric properties and other related parameters on the offset. We believe such investigations can furnish further insight into the mechanism.

In this article, we aim to gain a deeper understanding of the conditions under which sizable polarization offset occurs by studying the various dependences of the polarization shift. We demonstrate that the vertical shift along the displacement axis is strongly dependent on the remanent polarization and permittivity gradients, charge mobilities, and thickness in the graded ferroelectric thin film. Investigation on the charge motions and the time development of charge offsets further supports our previous notion that electric conduction asymmetry accounts for the shift of the hysteresis loop along the polarization axis.

^{a)}Electronic mail: zhou.yan@polyu.edu.hk

II. THEORY AND MODELING

A. Landau-Khalatnikov kinetics of switching

The graded ferroelectric film is considered as a stacking of N thin layers, each of thickness $\Delta x=L/N$, where L is the film thickness. We take $x=0$ at the interface between the ferroelectric film and the top electrode so that the position of any layer inside the film is given by $x=i\Delta x$, where $1\leq i\leq N$. The polarization and electric field at position x and time t are, respectively, denoted as $P(x,t)$ and $E(x,t)$, and are defined to be along the x direction. The dynamics of the dipoles is modeled by the Landau-Khalatnikov equation,

$$\gamma \frac{\partial P(x,t)}{\partial t} = -\alpha(x)P(x,t) - \beta(x)P(x,t)^3 + E(x,t) + \kappa(x) \times [P(x+\Delta x,t) + P(x-\Delta x,t) - 2P(x,t)], \quad (1)$$

where γ represents the viscosity that causes the delay in motion of dipole moments. $\alpha(x)<0$ and $\beta(x)>0$ are the corresponding Landau coefficients of the material at location x . The last term in Eq. (1) comes from the energy associated with polarization gradients, where $\kappa(x)$ is the corresponding interaction coefficient between neighboring dipoles.

The kinetic equation above conforms to the equations used by a number of works, notably Refs. 7–9, which is obtained by minimizing the free energy of the film under an applied electric field. It should be noted that $E(x,t)$ in Eq. (1) denotes the local electric field instead of the external electric field. With this approach, the explicit consideration of the depolarization field is subsumed in the formulation. In particular, Baudry and Tournier⁷ have given an excellent discussion on this point, incorporating implications due to the presence of charge carriers and the nonuniformity of polarization.

A more complete expression for Eq. (1) should include the corresponding terms from the elastic energy in the free energy of the system as is done in Ref. 10. However, for the case of the compositionally graded film investigated in the present work, the contribution of the elastic energy is found to be quite insignificant by following a calculation based on the relevant equations derived in Ref. 10. Therefore we neglected the elastic energy term in this work for simplicity.

The variables in Eq. (1) are then normalized to dimensionless variables by the following relations:

$$P^* = \frac{P}{P_S}, \quad t^* = \frac{t}{\tau}, \quad x^* = \frac{x}{\Delta x}, \quad (2)$$

$$\alpha^* = \frac{\tau\alpha}{\gamma}, \quad \beta^* = \frac{\tau P_S^2 \beta}{\gamma}, \quad E^* = \frac{\tau E}{\gamma P_S}, \quad \kappa^* = \frac{\tau\kappa}{\gamma},$$

where P_S is the remanent polarization for the ferroelectric thin film and τ is a characteristic relaxation time for the system. With normalized polarization and time parameters, Eq. (1) becomes

$$\frac{dP^*(x^*,t^*)}{dt^*} = -\alpha^*(x^*)P^*(x^*,t^*) - \beta^*(x^*)P^*(x^*,t^*)^3 + E^*(x^*,t^*) + \kappa^*(x^*)[(P^*(x^*+1,t^*) + P^*(x^*-1,t^*) - 2P^*(x^*,t^*)]. \quad (3)$$

B. Electric conduction

In our previous study of compositionally graded ferroelectric films,¹¹ we derived the following formula for the time-dependent conductivity associated with space charges and named it “time-dependent space-charge-limited conduction” (TDSCL):

$$\sigma(x,t) = \frac{\mu_p - \mu_n}{2} \frac{\partial D(x,t)}{\partial x} + \sqrt{\left[\frac{\mu_p + \mu_n}{2} \frac{\partial D(x,t)}{\partial x} \right]^2 + \sigma_0(x)^2}, \quad (4)$$

where $D(x,t)=\varepsilon(x)E(x,t)+P(x,t)$ is the electric displacement at position x , $\sigma_0(x)$ is the intrinsic conductivity, and μ_p and $-\mu_n$ ($\mu_p, \mu_n>0$) are the positive and negative charge-carrier mobilities, respectively. Here we also employ the same conduction mechanism as described in Ref. 7. The total current $J(t)$ across the circuit is constitutive of the conduction and displacement currents,

$$J(t) = j_c(x,t) + j_d(x,t) = \sigma(x,t)E(x,t) + \frac{\partial}{\partial t} D(x,t), \quad (5)$$

where the subscripts c and d denote the conduction and displacement currents, respectively. The circuit condition is given by

$$\int_0^L E(x,t)dx = V_0(t), \quad (6)$$

where L is the film thickness and $V_0(t)=V_{\text{amp}}\sin(\omega t)$ is the applied sinusoidal voltage. The measured charge density (accumulated on an ideal reference capacitor in a Sawyer-Tower circuit or by the use of the charge integration technique) at a certain time t_0 is given by the integration of total current density across the film,

$$Q(t_0) = \int_0^{t_0} J(t)dt. \quad (7)$$

The above variables are converted into dimensionless variables in the simulation by Eq. (2) together with the following relations:

$$D^* = \frac{D}{P_S}, \quad \varepsilon^* = \frac{\gamma\varepsilon}{\tau}, \quad j^* = \frac{\tau j}{P_S}, \quad V^* = \frac{\tau V}{\gamma\Delta x P_S}, \quad (8)$$

$$\sigma^* = \gamma\sigma, \quad \mu_p^* = \frac{P_S\gamma\mu_p}{2\Delta x}, \quad \mu_n^* = \frac{P_S\gamma\mu_n}{2\Delta x}, \quad Q^* = \frac{Q}{P_S}.$$

Equations (4) and (5) become

TABLE I. The dimensionless parameters used in our calculations.

Fig.	P_r^*	E_c^*	$\varepsilon^*/\varepsilon_0(10^{-2})$	$\sigma_0^*(10^{-4})$	L^*	$\mu_p^*(10^{-3})$	μ_n^*
1	0.3+0.04x	0.2	2.6+0.033x	1	30	0.01	0.1
2(a)	0.3+0.04x	0.3	2.6+0.033x	2	30	0.01	0.1
2(b)	1.5-0.04x	0.3	3.6-0.033x	2	30	0.01	0.1
2(c)	0.3+0.04x	0.3	3.6-0.7x+0.0222x ²	2	30	0.01	0.1
2(d)	1.5-0.04x	0.3	2.6-1.3x+0.0444x ²	2	30	0.01	0.1
3(a)	0.3+0.04x	0.3	2.6+0.033x	2	30	0.01	0.5
3(b)	0.3+0.04x	0.3	2.6+0.033x	2	30	0.01	0.01
4(a)	0.3+0.04x	0.3	2.6+0.033x	2	20	0.01	0.1
4(b)	0.3+0.04x	0.3	2.6+0.033x	2	100	0.01	0.1
5	0.3+0.04x	0.3	2.6+0.033x	2	30	0.01	0.1

$$\sigma^*(x^*, t^*) = (\mu_p^* - \mu_n^*) \frac{\partial D^*(x^*, t^*)}{\partial x^*} + \sqrt{\left[(\mu_p^* + \mu_n^*) \frac{\partial D^*(x^*, t^*)}{\partial x^*} \right]^2 + \sigma_0^*(x^*)^2}, \quad (9)$$

$$J^*(t^*) = j_c^*(x^*, t^*) + j_d^*(x^*, t^*) = \sigma^*(x^*, t^*) E^*(x^*, t^*) + \frac{\partial}{\partial t^*} D^*(x^*, t^*). \quad (10)$$

Also, the form of Eqs. (6) and (7) does not change if written in terms of the dimensionless variables.

We have chosen the following values of the parameters: $f^* = 0.02$ and $E_{\text{amp}}^* = 1.5$ (which, e.g., correspond to $f = 1$ kHz and $E_{\text{amp}} = 150$ kV/cm for the graded PZT thin film) for the calculations, where $E_{\text{amp}}^* = V_{\text{amp}}^*/L^*$ is the normalized applied electric-field amplitude, while $L^* = L/\Delta x$ is the normalized film thickness. Unless stated otherwise, these values have been retained for obtaining all of the results presented in this paper. Also, it is found through calculation that the effects of $\kappa(x)$ on the results are quite limited. Hence we have neglected $\kappa(x)$ in the simulation. All the modeled results are picked from the application time to the sixth cycle of the external ac field to examine the shift effect.

III. RESULTS AND DISCUSSION

The purpose of this paper is to gain a deeper understanding of the conditions under which large polarization offset occurs or otherwise. The selection of parameters in fitting a particular experiment is based on the relations in Eqs. (2) and (8). The parameters used in our modeling are listed in Table I, where ε_0 is the permittivity of vacuum.

A. Effects of polarization and permittivity gradients

The anomalous vertical offset of hysteresis loops are usually observed in graded ferroelectric films (e.g., temperature or compositionally graded). For these kinds of materials, the ferroelectric, dielectric, and electric properties may vary across the thickness due to the composition gradient or to any other stimulus (temperature, mechanical stress, etc.). Investigation of the critical variables which have to be graded to lead to the offsets can help in understanding the rather complicated anomalous shift mechanism. Figure 1 shows the

downward shifting loops when only P_r^* and ε^* are linearly increasing across the film thickness direction. Our simulations show that the remanent polarization and permittivity gradients are already sufficient to demonstrate the shift phenomenon. Figure 2(a) is obtained with the same P_r^* and ε^* gradients but different E_c^* and σ_0^* as in Fig. 1. Furthermore, it is found that E_c^* and σ_0^* gradients (e.g., we have tried 0.1–2 for both E_c^* and σ_0^* gradients) do not impose any significant effects on the final results. It is also found that being graded only in either ε^* or P_r^* is not sufficient to lead to the vertical offset.

We have numerically validated that E_c^* and σ_0^* gradients do not lead to nor sensitively affect offsets. We therefore assume E_c^* and σ_0^* to be constant in the following calculations for simplicity. On inverting the P_r^* and ε^* gradient directions (decreasing with x^*), it is found that the vertical shifting is in the upward direction, as shown in Fig. 2(b). The vertical shifting effect will become more notable for larger gradients of P_r^* and ε^* . Interestingly, there is no shifting effect at all if the uniform gradients of remanent polarization and permittivity are in opposite directions. The loops will only display a vertical shift with nonlinear permittivity variation across the thickness direction for this opposing gradients case. Here we used a simple quadratic function to describe the permittivity profile (Table I). Figure 2(c) shows the downward shifting loops with linearly increasing P_r^* but nonlinearly de-

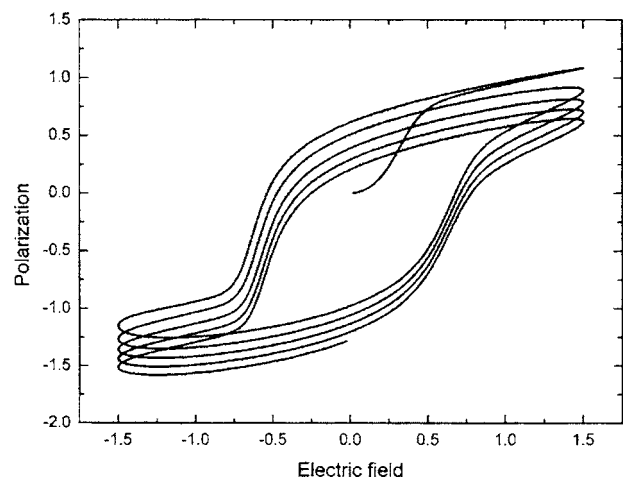


FIG. 1. The shifting of hysteresis loops when only P_r^* and ε^* are linearly increasing with x^* .

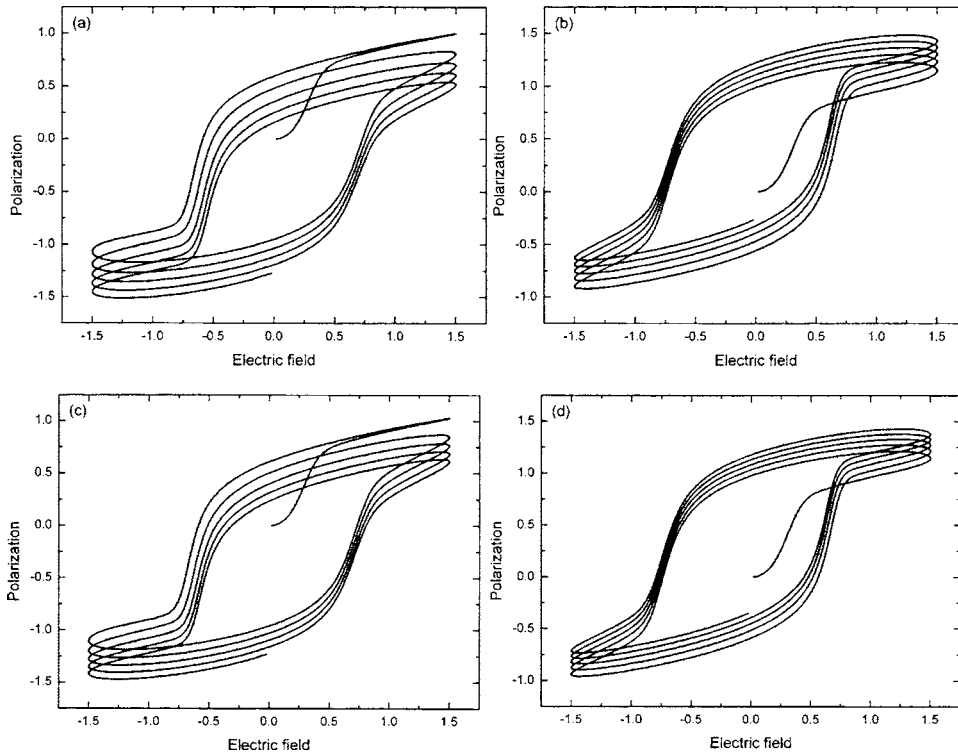


FIG. 2. The shifting of hysteresis loops (a) with linearly increasing P_r^* and ε^* gradients, (b) with linearly decreasing P_r^* and ε^* gradients, (c) with linearly increasing P_r^* gradient but nonlinearly decreasing ε^* gradient, and (d) with linearly decreasing P_r^* gradient but nonlinearly increasing ε^* gradient along the film thickness direction.

creasing ε^* along the film thickness direction. Similarly, the simulated upward shifting hysteresis loops shown in Fig. 2(d) are calculated with linearly decreasing P_r^* but nonlinearly increasing ε^* along the film thickness direction. From the above simulation results, we can see that the shifting direction is mostly determined by the gradient direction of P_r^* . The polarization offset is positive (negative) with negative (positive) P_r^* gradient. This point is validated by experimental results reported in the literature.^{12–15}

B. Effect of charge-carrier mobilities and film thickness

The phenomena of asymmetric leakage current have been observed in many thin-film materials, and it has been theoretically demonstrated that space charges are likely responsible for the occurrence of polarization offsets in graded ferroelectrics. The purpose of this section is to investigate the effects of free charge-carrier mobilities on the anomalous hysteretic behavior in graded thin films. In this calculation, the remanent polarization and permittivity are assumed to be linearly varying with x in the same direction. Figures 3(a) and 3(b) show the simulated hysteresis loops by adopting different negative charge-carrier mobilities. As μ_n^* decreases, the vertical “shift” decreases. It is interesting to note that the modeled hysteresis loop is very symmetrical and centered at the origin of the axes when the mobility is small enough (e.g., $\mu_n^*=0.01$). It is also found that when μ_n^* is smaller than μ_p^* by an order, an almost maximum vertical shift is observed. Any further reduction in μ_p^* will have little effect in the vertical shift. When the values for μ_p^* and μ_n^* are interchanged, the hysteresis loop shifts to the opposite direction with an almost unchanged shift magnitude after a certain number of cycles.

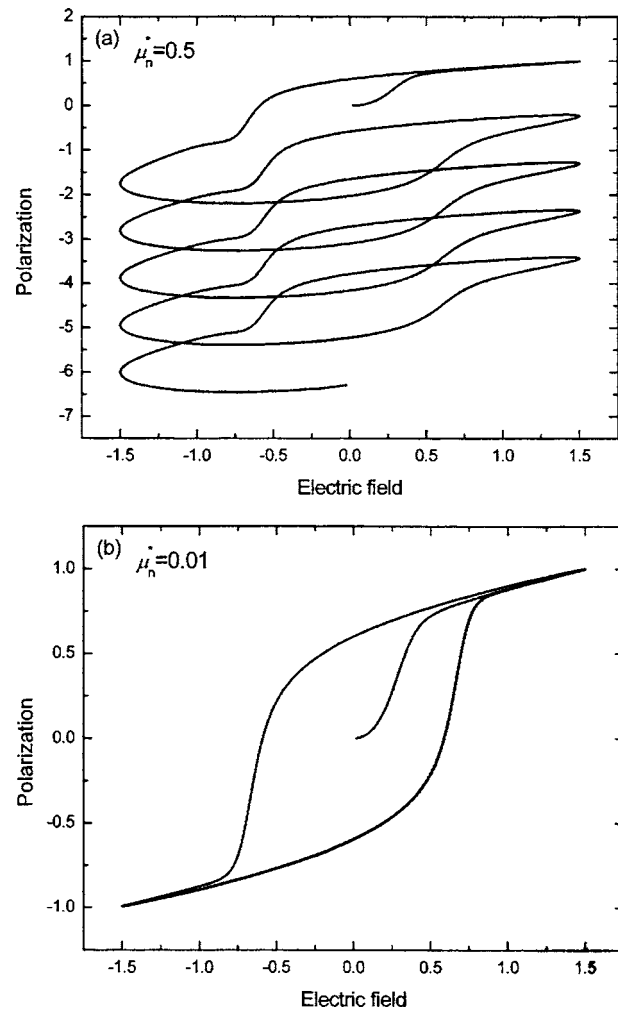


FIG. 3. The simulated hysteresis loops (a) when $\mu_n^*=0.5$, and (b) when $\mu_n^*=0.01$.

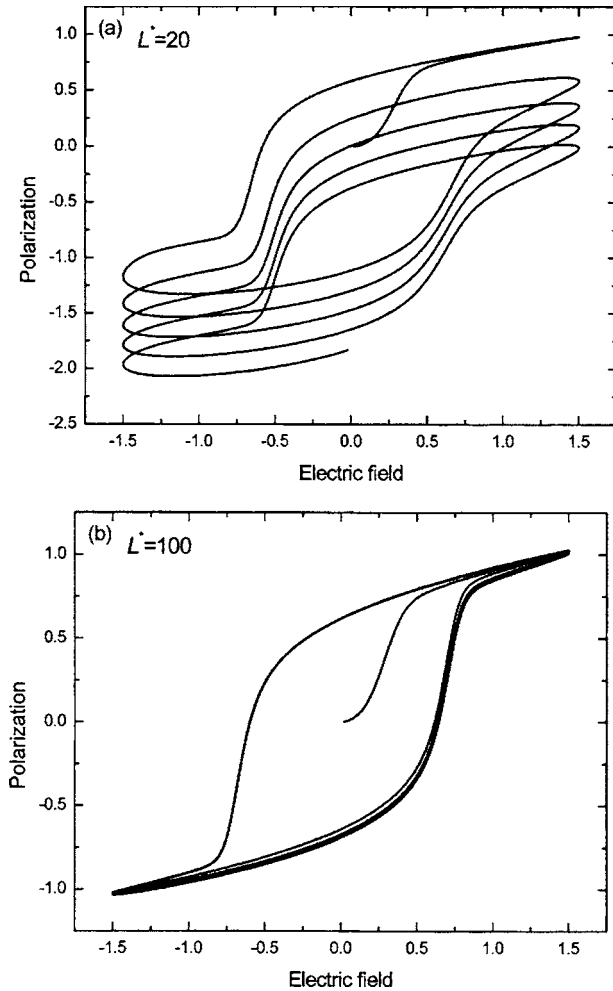


FIG. 4. Effect of thickness of ferroelectric thin film on the simulated hysteresis loops (a) when $L^* = 20$, and (b) when $L^* = 100$.

Figure 4 shows the effect of film thickness on the hysteresis loops. As the thickness increases, the vertical shift decreases. There is almost no vertical shift when the film is thick enough (e.g., $L^* = 100$). In fact, it is found that there will be notable polarization offset only when the thickness lies between 10 nm and 3 μm by modeling the compositionally graded PZT thin film. This is also the range of experimental measurements where notable vertical shifts of the hysteresis loop are reported in the literature.¹²⁻¹⁵

In our previous study of compositionally graded ferroelectric films, we have already demonstrated that the polarization gradient across a ferroelectric film can lead to asymmetric conduction, which we believe provides a mechanism for the polarization offset phenomenon. Now it is worth further examining the asymmetric conduction current. From Eqs. (4) and (6), we can see that the charge offset $Q^*(t^*)$ should come from either or both of the two parts: one is the conduction-current-induced charge accumulation $Q_c^*(x^*, t^*) = \int_0^{t^*} J_c(x^*, t^*) dt^*$; the other is the displacement-current-induced charge accumulation $Q_d^*(x^*, t^*) = \int_0^{t^*} J_d(x^*, t^*) dt^*$. Figure 5 shows the time development of Q_c^* , Q_d^* , and the total Q^* . From the figure, it is evident that the displacement-current-accumulated charge Q_d^* repeats itself quite well in successive field cycles while the conduction-current-induced

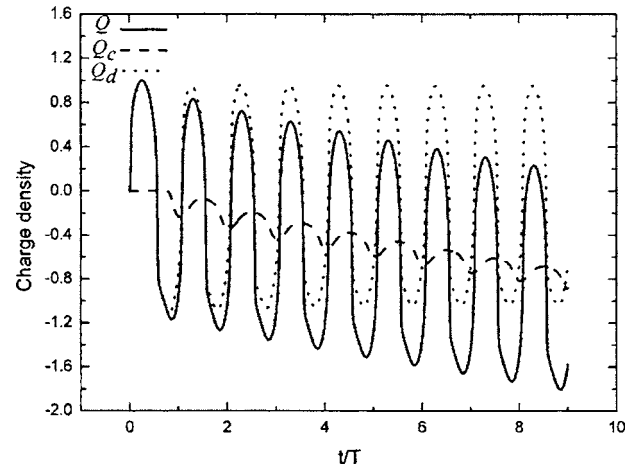


FIG. 5. Time development of charge densities induced by the conduction, displacement, and total currents.

charge Q_c^* develops to larger negative values with time. It is therefore obvious that the charge offset comes mostly from the conduction-current-induced charge accumulation Q_c^* . Hence the simulation results confirm our previous notion that the asymmetric electric conduction mechanism is a major contributor to the polarization offsets observed in experiments.

Summing up, the above simulation results show that apart from polarization and permittivity gradients, the effects of charge-carrier mobility and film thickness are also important factors determining the vertical offset behavior. Although the cases discussed here are simplified and not exhaustive, they, however, represent reasonable first approximations to some possible variation in properties within realistic graded ferroelectric films [e.g., both P_r and ϵ are almost linearly varied with Zr concentration for the continuous compositionally graded $\text{Pb}(\text{Zr}_y\text{Ti}_{1-y})\text{O}_3$ ferroelectric structures where y varies from 0.2 to 0.56]. In fact, a linearly graded polarization assumption is also adopted by Pintilie *et al.*⁶ Our results indicate that the effect of vertical offset can be enhanced by the following conditions:

- (1) The remanent polarization and permittivity gradients are in the same direction and large enough within the graded ferroelectric;
- (2) Either the positive or negative charge mobility is reasonably large, with a nonzero difference between them; and
- (3) The film should be thin enough, e.g., $\leq 3 \mu\text{m}$ for PZT.

Our simulation results are valid for the film with a continuous gradient, but should also be valid for films in which polarization increases or decreases in steps from one layer to the other. This study has provided direction for obtaining large vertical offsets in graded ferroelectric thin films for developing new applications. However, further efforts are required to understand the detailed charge dynamics of the shift mechanism.

ACKNOWLEDGMENT

The authors acknowledge the support of an internal grant from The Hong Kong Polytechnic University.

- ¹N. W. Schubring, J. V. Mantese, A. L. Micheli, A. B. Catalan, and R. J. Lopez, *Phys. Rev. Lett.* **68**, 1778 (1992).
- ²S. P. Alpay, Z. G. Ban, and J. V. Mantese, *Appl. Phys. Lett.* **82**, 1269 (2003).
- ³J. V. Mantese, N. W. Schubring, A. L. Micheli, M. P. Thompson, R. Naik, G. W. Auner, I. B. Misirlioglu, and S. P. Alpay, *Appl. Phys. Lett.* **81**, 1068 (2002).
- ⁴F. Jin, G. W. Auner, R. Naik, N. W. Schubring, J. V. Mantese, A. B. Catalan, and A. L. Micheli, *Appl. Phys. Lett.* **73**, 2838 (1998).
- ⁵G. Poullain, R. Bouregba, B. Vilquin, G. L. Rhun, and H. Murray, *Appl. Phys. Lett.* **81**, 5015 (2002).
- ⁶L. Pintilie, I. Boerasu, and M. J. M. Gomes, *J. Appl. Phys.* **93**, 9961 (2003).
- ⁷L. Baudry and J. Tournier, *J. Appl. Phys.* **90**, 1442 (2001).
- ⁸L. Baudry, *J. Appl. Phys.* **86**, 1096 (1999).
- ⁹V. C. Lo, *J. Appl. Phys.* **94**, 3353 (2003).
- ¹⁰Z. G. Ban, S. P. Alpay, and J. V. Mantese, *Phys. Rev. B* **67**, 184104 (2003).
- ¹¹H. K. Chan, C. H. Lam, and F. G. Shin, *J. Appl. Phys.* **95**, 2665 (2004).
- ¹²M. Brazier, M. McElfresh, and S. Mansour, *Appl. Phys. Lett.* **72**, 1121 (1998).
- ¹³D. Bao, N. Wakiya, K. Shinozaki, N. Mizutani, and X. Yao, *J. Appl. Phys.* **90**, 506 (2001).
- ¹⁴R. Bouregba, G. Poullain, B. Vilquin, and G. L. Rhun, *J. Appl. Phys.* **93**, 5583 (2003).
- ¹⁵M. Brazier, M. McElfresh, and S. Mansour, *Appl. Phys. Lett.* **74**, 299 (1999).